Electron Spin Decoherence in Bulk and Quantum Well Zincblende Semiconductors

Wayne H. Lau, J. T. Olesberg, and Michael E. Flatté

Department of Physics and Astronomy, University of Iowa, Iowa City, IA 52242

Abstract

A theory for longitudinal (T_1) and transverse (T_2) electron spin coherence times in zincblende semiconductor quantum wells is developed based on a non-perturbative nanostructure model solved in a fourteen-band restricted basis set. Distinctly different dependences of coherence times on mobility, quantization energy, and temperature are found from previous calculations. Quantitative agreement between our calculations and measurements is found for GaAs/AlGaAs, InGaAs/InP, and GaSb/AlSb quantum wells.

The recent observation of long-lived (> 100 ns) spatially extended (> 100 μm) coherent spin states in semiconductors suggests the possibility of manipulating nonequilibrium electron coherence to an unprecedented degree in a solid. [1–4] These spin states interact with light, and thus can be used to generate a host of novel dynamic nonlinear optical and electrical effects. [5] The magnitude and persistence of such effects is governed partly by the spin coherence times T_1 and T_2, describing the decay of longitudinal and transverse spin order, respectively. Ultrafast optical measurements have been performed of both T_1 and T_2, although in different geometries [2–4,6–10].

To guide further efforts in the controllable manipulation of room-temperature spin coherence it is essential to have a *quantitative* theory of spin decoherence. Direct quantitative comparison of the current theory with experiment has been rare for quantum wells, for an independent measurement of the mobility of the quantum well is required. Recently such a comparison was made for room-temperature electron spin lifetimes in n-doped GaAs/AlGaAs multiple quantum wells (MQWs) [8]. In addition to measured T_1's one order of magnitude longer than those predicted from current theory there were discrepancies in the power law dependences of T_1 on mobility and confinement energy.

This Letter provides the desired quantitatively accurate theory of spin decoherence for quantum wells and clarifies the relationship between T_1 and T_2 in these systems. Our results are in excellent agreement with experimental measurements on GaAs quantum wells [8], not only in the previously unexplained general trends, but also in the absolute magnitude. We also find excellent agreement with measurements on InGaAs/InP [9] and GaSb/AlSb [10] quantum wells, whereas previous calculations disagree by an order of magnitude. Finally we find unexpected trends in the spin coherence times with temperature which may explain other puzzling experimental results.

The mechanism of electron spin decoherence we consider occurs via the spin precession of carriers with finite crystal momentum $\mathbf{k}$ in the effective $\mathbf{k}$-dependent crystal magnetic field of an inversion-asymmetric material. A signature of this mechanism is that in the "motional narrowing" regime, where orbital scattering times τ greatly exceed spin decoherence times, $T_1 \propto \tau^{-1}$. Thus cleaner samples have shorter spin coherence times. In III-V bulk [11] and quantum well structures [8] nanostructures this trend has been observed in samples of varying mobility at and near room temperature.

D'yakonov and Perel' have developed a theory for T_1 based on this mechanism for bulk zincblende semiconductors, assuming orbital coherence is lost after each scattering event, and assuming a thermal distribution of electrons [12]. This work was later extended (with further approximations) to quantum wells [13] by D'yakonov and Kachorovskii (DK). Thus the two categories of approximation in DK theory are (1) the method of handling the orbital degrees of freedom and (2) the quantum well electronic structure. For example, if some *orbital* coherence or nonthermal occupation were maintained after each scattering event, then because the electron's orbital degrees of freedom are entangled with its spin, only a nonequilibrium calculation of orbital degrees of freedom (e.g. Monte Carlo) would produce accurate results. We find, however, that the sources of error are the approximations pertaining to quantum well electronic structure, and thus simpler, *quantitatively accurate* calculations of spin coherence may be performed.

Our theory begins with the assumption of motional narrowing. In the motional narrowing regime the electronic spin system is subject to an effective *time-dependent,* randomly oriented

magnetic field $\mathbf{H}$ which changes direction with a time τ that is much shorter than the precession time of either the constant applied field $\mathbf{H_o}$ or the random field. The coherence times depend on the transverse ($H_\perp$) and longitudinal ($H_\parallel$) components of the random field, according to [14]

$$T_1^{-1} \propto (H_\perp^2)\tau, \tag{1}$$
$$T_2^{-1} \propto ([H_\perp^2]/2 + H_\parallel^2)\tau, \tag{2}$$

where the constant of proportionality is the same for Eqs. (1) and (2). In a crystal with inversion asymmetry and spin-orbit coupling there is a spin splitting described by the Hamiltonian $H = \hbar\mathbf{\Omega}(\mathbf{k}) \cdot \sigma/2$, where $\mathbf{\Omega}(\mathbf{k})$ is a *momentum-dependent* effective magnetic field. As the electron is scattered from $\mathbf{k}$ to $\mathbf{k}'$ via ordinary orbital (not spin-dependent) elastic scattering, the effective magnetic field changes direction with time. If the crystal is cubic, then $H_x^2 = H_y^2 = H_z^2$, so $H_\perp^2 = 2H_\parallel^2$ and $T_2 = T_1$. The relationship between T_1 and T_2 differs, however, for systems of lower symmetry, such as quantum wells. For a (001) grown quantum well the fluctuating field along the growth direction vanishes, and

$$T_1^{-1}(\alpha) = T_1^{-1}(\alpha = 0)(1 + \cos^2\alpha)/2, \tag{3}$$
$$T_2^{-1}(\alpha) = T_1^{-1}(\alpha = 0)(2 + \sin^2\alpha)/4, \tag{4}$$

where α is the direction between $\mathbf{H_o}$ and the growth direction. Thus T_2 ranges from $2T_1/3$ to $2T_1$ depending on α. In contrast, for (110) grown quantum wells the effective crystal magnetic field is entirely along the growth direction, and

$$T_1^{-1}(\alpha) = T_2^{-1}(\alpha = 0)\sin^2\alpha, \tag{5}$$
$$T_2^{-1}(\alpha) = T_2^{-1}(\alpha = 0)(1 + \cos^2\alpha)/2. \tag{6}$$

Thus although $T_1^{-1}(\alpha = 0)$ vanishes, the same is not the case for T_2^{-1} for any α.

Calculations of T_1 require knowledge of both τ and $\mathbf{\Omega}(\mathbf{k})$. The effective time for field reversal (τ_ℓ) depends on the angular index ℓ of the field component (Ω_ℓ). For example, an $\ell = 1$ component (Ω_1) requires a 180° change in the angle of $\mathbf{k}$ to change sign, whereas an $\ell = 3$ component (Ω_3) only requires a 60° change, so typically $\tau_3 < \tau_1$. Thus

$$\frac{1}{T_1} = \frac{1}{n}\int D(E)f(E)[1 - f(E)]\sum_\ell \tau_\ell(E)\Omega_\ell^2(E)dE, \tag{7}$$

where $f(E)$ is the Fermi occupation function, $D(E)$ is the density of states, n is the electron density, and the scattering rates $\tau_\ell^{-1}(E) = \int_{-1}^{1}\sigma(\theta, E)(1 - P_\ell(\cos\theta))d\cos\theta$ for bulk semiconductors and $\tau_\ell^{-1}(E) = \int_0^{2\pi}\sigma(\theta, E)(1 - \cos[\ell\theta])d\theta$ for (001) quantum wells. For both bulk and quantum wells the functional form of the scattering cross-section $\sigma(\theta, E)$ is taken from standard expressions for ionized impurity (II), neutral impurity (NI — such as arises from quantum well interface roughness), or optical phonon (OP) scattering. The τ_ℓ's differ for different mechanisms (e.g., for a quantum well $\tau_1/\tau_\ell = \ell^2$ for II, $\tau_1/\tau_\ell = \ell$ for OP, and $\tau_1/\tau_\ell = 1$ for NI scattering). The magnitude of $\sigma(\theta, E)$ is obtained from the mobility,

$$\mu = (e/mn)\int D(E)f(E)[1 - f(E)]\tau_1(E)EdE. \tag{8}$$

We obtain $\Omega_\ell(E)$ from a non-perturbative calculation in a fourteen-band basis [15]. This basis, which is the minimum required to generate spin splitting nonperturbatively, consists of two conduction antibonding s states ($\overline{s}$), six valence (bonding) p states, and six antibonding p states ($\overline{p}$). Such a basis has, for example, been used to analyze spin-splitting in heterostructures [16]. The Hamiltonian is well-known, and can be found in Refs. [17,15]. The parameters that enter this Hamiltonian include the zone-center energies of the constituent bulk semiconductors and the momentum matrix elements between bands, which are obtained from the conduction band mass, the heavy-hole mass, and the g-factor. Time reversal invariance requires $\mathbf{\Omega}(\mathbf{k}) = -\mathbf{\Omega}(-\mathbf{k})$, so $\Omega_\ell = 0$ for even ℓ.

For quantum wells the electronic structure is obtained by expressing the electronic states as spatially-dependent linear combinations of the fourteen states in the basis. The full Hamiltonian is projected onto this restricted basis set, which produces a set of fourteen coupled differential equations for the spatially-dependent coefficients of the basis states (generalized envelope functions). These equations are then solved in Fourier space in a similar method to that of Winkler and Rössler. [18] Further details are available elsewhere [15].

For bulk semiconductors the relevant electronic states for spin decoherence are near the bulk band edge, and thus perturbative expressions for $\Omega_\ell^2(E)$ for these bulk semiconductors ($\Omega_1^2(E) = 0$, $\Omega_3^2(E) \propto E^3$) [12] are identical to those obtained from a full fourteen-band calculation within numerical accuracy. Shown in Fig. 1 are calculated T_2's for GaAs, InAs, and GaSb assuming II scattering. The agreement with experimental measurements [3] for GaAs at the higher temperatures is quite good, whereas for low temperatures other spin relaxation mechanisms are expected to dominate. The smaller T_2's in InAs and GaSb are due partly to the larger conduction spin splitting, which originates from a larger ratio of the spin-orbit coupling Δ to the band gap E_g (see Ref. [19] on perturbative expansions of spin splittings). The agreement between calculated and measured T_2's in Fig. 1 indicates that the spin splitting of bulk GaAs is well described by our model.

We now contrast our results for quantum wells with those of DK theory. The DK theory for (001) quantum wells is derived as follows. First, negligible penetration of the electronic states into the barriers is assumed, so $E_1 \ll \Delta E_c$, where E_1 is the confinement energy of the first quantum well state and ΔE_c is the conduction band offset. Then the perturbative expressions [20] $\Omega_1^2(E) \propto E(4E_1 - E)^2$ and $\Omega_3^2(E) \propto E^3$ are used. Furthermore the energies of relevant states are assumed to be $\ll E_1$, and thus *(i)* the contribution from $\Omega_3(E)$ is ignored, and *(ii)* it is assumed that $\Omega_1^2(E) \propto E$. It is not generally recognized that the conditions $kT \ll E_1 \ll \Delta E_c$ are quite restrictive and are difficult to satisfy at room temperature.

The resulting T_1^{-1} [Eq. (7)] under the DK assumptions is proportional to the mobility *independent of the dominant scattering mechanism* [see Eq. (8)]. In addition, T_1^{-1} is proportional to E_1^2. These trends are not supported by recent experimental measurements [8,21] on 75Å n-doped GaAs/$Al_{0.4}Ga_{0.6}$As MQWs at 300K [shown in Fig. 2(a,b) (filled circles)]. In both cases the experimental trends are weaker than the predicted theoretical ones. Calculations are shown in Fig. 2(a,b) based on our more general theory using OP (solid line) and NI (dashed line) as the dominant process determining the mobility.

Our results agree with experiment if one assumes a shift from OP to NI scattering as the mobility drops — this is the origin of the unusual experimental dependence of T_1 on the mobility. The weaker dependence of T_1 on E_1 in our theory versus DK theory in Fig. 2(b) is due to wavefunction penetration into the barriers and non-perturbative effects.

We emphasize as well the key role of temperature studies of the mobility in analyzing the temperature dependence of spin coherence. In Fig. 2(c) the calculated T_1 for one sample with a given room-temperature mobility is presented as a function of temperature for NI and OP scattering. In particular the OP results appear relatively insensitive to temperature from 100-250K — this is due to the rapid decrease in the mobility from OP scattering with increasing temperature. This may play a role in the weak temperature dependence seen in Ref. [2].

Figure 3 compares the energy dependence of $\Omega_1^2(E)$ and $\Omega_3^2(E)$ for several additional material systems. The cubic dependence of $\Omega_3^2(E)$ for the three bulk semiconductors is confirmed in Fig. 3(a). Fig. 3(b), however, shows that for quantum wells $\Omega_1^2(E)$ is only linear (short dashed line for the GaAs MQW) for a small energy range ($\sim$ 20 meV) above the band edge before it begins to deviate. More energetic states than this certainly contribute to the spin coherence times at room temperature. The wider the well the lower the energy where $\Omega_1^2(E)$ deviates from linear behavior, as it approaches a bulk-like E^3 behavior. $\Omega_3^2(E)$ for these structures is shown in Fig. 3(c), and is comparable in magnitude to $\Omega_1^2(E)$. As the wells become narrower, even the perturbative expressions for Ω_3 and Ω_1 break down. Figure 3(d) shows $\Omega_1^2(E)$ and $\Omega_3^2(E)$ for a thin-layer InAs/GaSb superlattice, indicating very different behavior from the other structures, poorly reproduced by even the general forms of the perturbative expression.

Table I presents calculations and experimental measurements of T_1 for these material systems. The order of magnitude discrepancy between DK calculations and measurements occurs here as well. Given the uncertainty in experimental mobilities and densities, the agreement of our calculations with experiment for both NI and OP scattering is good for all systems, and is much better than DK theory. Note that OP and NI scattering calculations in the full theory differ from each other by factors of of up to 2 (due to differences in $\tau_\ell(E)$), whereas all scattering mechanisms produce the same result in DK theory. As expected, for several systems the T_1's are much shorter at higher electron densities, for as the carrier distribution is spread further from zone center the effective crystal magnetic fields increase. The DK approximation *(i)* can be evaluated by comparing OP_1 to OP and NI_1 to NI, where calculations using all terms up to ℓ are designated OP_ℓ and NI_ℓ. The difference is up to 40%. Approximation *(ii)*, however, produces a discrepancy between the DK result and both NI_1 and OP_1 which can greatly exceed an order of magnitude.

These calculations consider decoherence arising from the bulk inversion asymmetry (BIA) of the constituent materials. We have considered symmetric wells, so another source of inversion asymmetry, the structural inversion asymmetry (SIA), does not play a role. In other structures, such as single-interface heterostructures, SIA may dominate [22]. Interface bonding asymmetry (native interface asymmetry, or NIA), which arises in non-common-atom structures, could play a role in systems II, IV, or V. The NIA spin splitting for perfect interfaces (imperfect interfaces reduce the NIA contribution) has been calculated for System II in Ref. [23]. By comparing with Ref. [23] we find the spin splitting of this quantum well is dominated by BIA.

We have presented a *quantitatively accurate* non-perturbative nanostructure theory for electron spin relaxation in bulk and quantum well zincblende semiconductors based on a fourteen band model. The calculated electron spin lifetimes in III-V semiconductor bulk and quantum well materials are in agreement with experimental measurements, indicating

the importance of accurate band structure calculations for zincblende type nanostructures.

We would like to acknowledge discussions with D. D. Awschalom, T. F. Boggess, J. M. Byers, J. M. Kikkawa, and A. Smirl. We would also like to thank D. D. Awschalom and J. M. Kikkawa for providing mobility data for the bulk GaAs sample of Ref. [3]. This work was supported in part by the Office of Naval Research through Grant No. N00014-99-1-0379.

REFERENCES

[1] D. Divincenzo, Science **270**, 255 (1995); L. Sham, *ibid*, **277**, 1258 (1997); G. Prinz, *ibid*, **282**, 1660 (1998); *ibid* **283**, 330 (1999).

[2] J. M. Kikkawa, I. O. Smorchkova, N. Samarth, and D. D. Awschalom, Science **277**, 1284 (1997).

[3] J. M. Kikkawa and D. D. Awschalom, Phys. Rev. Lett. **80**, 4313 (1998).

[4] J. M. Kikkawa and D. D. Awschalom, Nature (London) **397**, 139 (1999).

[5] E. Knill and R. Laflamme, Phys. Rev. Lett. **81**, 5672 (1999); J. Preskill, Phys. Today **52**, 24 (1999); J. M. Kikkawa and D. D. Awschalom, Science **287**, 473 (2000).

[6] J. Wagner, *et al.*, Phys. Rev. B **47**, 4786 (1993).

[7] R. S. Britton, *et al.*, Appl. Phys. Lett. **73**, 2140 (1998); J. T. Hyland, *et al.*, Semicond. Sci. Technol. **14**, 215 (1999).

[8] R. Terauchi, Y. Ohno, T. Adachi, A. Sato, F. Matsukura, A. Tackeuchi, and H. Ohno, Jpn. J. Appl. Phys. **38**, Pt. 1, No. 4B., 2549 (1999).

[9] A. Tackeuchi, O. Wada, and Y. Nishikawa, Appl. Phys. Lett. **70**, 1131 (1997); R. Tackeuchi, T. Kuroda, S. Muto, Y. Nishikawa, and O. Wada, Jpn. J. Appl. Phys. **38**, Pt. 1, No. 8, 4680 (1999).

[10] K. C. Hall, *et al.*, Appl. Phys. Lett. **75**, 3665 (1999); **75**, 4156 (1999).

[11] *Optical Orientation, Modern Problems in Condensed Matter Science*, edited by F. Meier and B. P. Zachachrenya (North-Holland, Amsterdam, 1984), Vol. 8.

[12] M. I. D'yakonov and V. I. Perel', Sov. Phys. JETP **33**, 1053 (1971); Sov. Phys. Solid State **13**, 3023 (1972).

[13] M. I. D'yakonov and V. Yu. Kachorovskii, Sov. Phys. Semicond **20**, 110 (1986).

[14] Y. Yafet in *Solid State Physics Vol. 14*, (Academic Press, New York, 1963), p. 1.

[15] J. T. Olesberg, Ph. D. thesis, University of Iowa, 1999.

[16] L. Wissinger, *et al.*, Phys. Rev. B **58**, 15375 (1998).

[17] P. Y. Yu and M. Cardona, *Fundamentals of semiconductors, Physics and materials properties*, 2nd ed. (Springer, New York 1999).

[18] R. Winkler and U. Rossler, Phys. Rev. B **48**, 8918 (1993).

[19] M. Cardona, N. E. Christensen, and G. Fasol, Phys. Rev B **38**, 1806 (1988).

[20] E. L. Ivchenko and G. E. Pikus, *Superlattices and Other Heterostructures*, 2nd ed. (Springer, New York, 1997).

[21] The experimental results have been adjusted from Ref. [8], for the authors defined an effective spin flip time for a single spin, $\tau_s = 2T_1$, and plotted their results for τ_s. The DK calculation (dot-dashed line) is of T_1, so in addition to the errors in trends, the discrepancy in the magnitude of T_1 (using our values of the confinement energy) is about a factor of 4 in Fig. 2(a,b).

[22] P. Pfeffer and W. Zawadzki, Phys. Rev. B **52**, R14332 (1995); P. Pfeffer, *ibid* **55**, R7359 (1997); P. Pfeffer and W. Zawadzki, *ibid* **59**, R5312 (1999).

[23] L. Vervoort, R. Ferreira, and P. Voisin, Semicond. Sci. Technol. **14**, 227 (1999).

[24] O. Madelung, *Semiconductors-Basic Data*, 2nd ed. (Springer, New York, 1996).

TABLES

TABLE I. Spin coherence times T_1 (ps) for several structures, I: a 75Å $GaAs/Al_{0.4}Ga_{0.6}As$ MQW [8], II: a 70Å $In_{0.53}Ga_{0.47}As$/97Å InP MQW [9], III: an 80Å GaSb/80Å AlSb MQW [10], IV: a 51Å $GaAs_{0.19}Sb_{0.81}$/80Å AlSb MQW [10], and V: a 21.2Å InAs/36.6Å GaSb superlattice. Calculated times are shown for a given total electron density (n.d. indicates nondegenerate) using DK theory (DK), and the nonperturbative theory with optical phonon (OP) and neutral impurity (NI) scattering. The subscript ℓ indicates that only terms up to Ω_ℓ were used in the calculation.

	System	Density (cm^{-3})	μ (cm^2/Vs)	Exp.	DK	OP_1	OP	NI_1	NI
I	GaAs/AlGaAs	2.7×10^{17}	800	100	27	151	120	162	111
II	InGaAs/InP	n.d.	6700	—	1.45	53	37	52	32
		3.0×10^{18}	6700	2.6	0.21	6.0	4.9	6.9	4.0
III	GaSb/AlSb	n.d.	2000	—	0.59	1.9	1.8	1.5	1.4
		2.8×10^{18}	2000	0.52	0.09	0.64	0.55	0.88	0.53
IV	GaAsSb/AlSb	n.d.	2000	—	0.09	0.53	0.52	0.44	0.43
		3.4×10^{18}	2000	0.42	0.01	1.9	1.4	1.7	0.87
V	InAs/GaSb	n.d.	3000	—	0.38	0.77	0.77	1.7	1.6

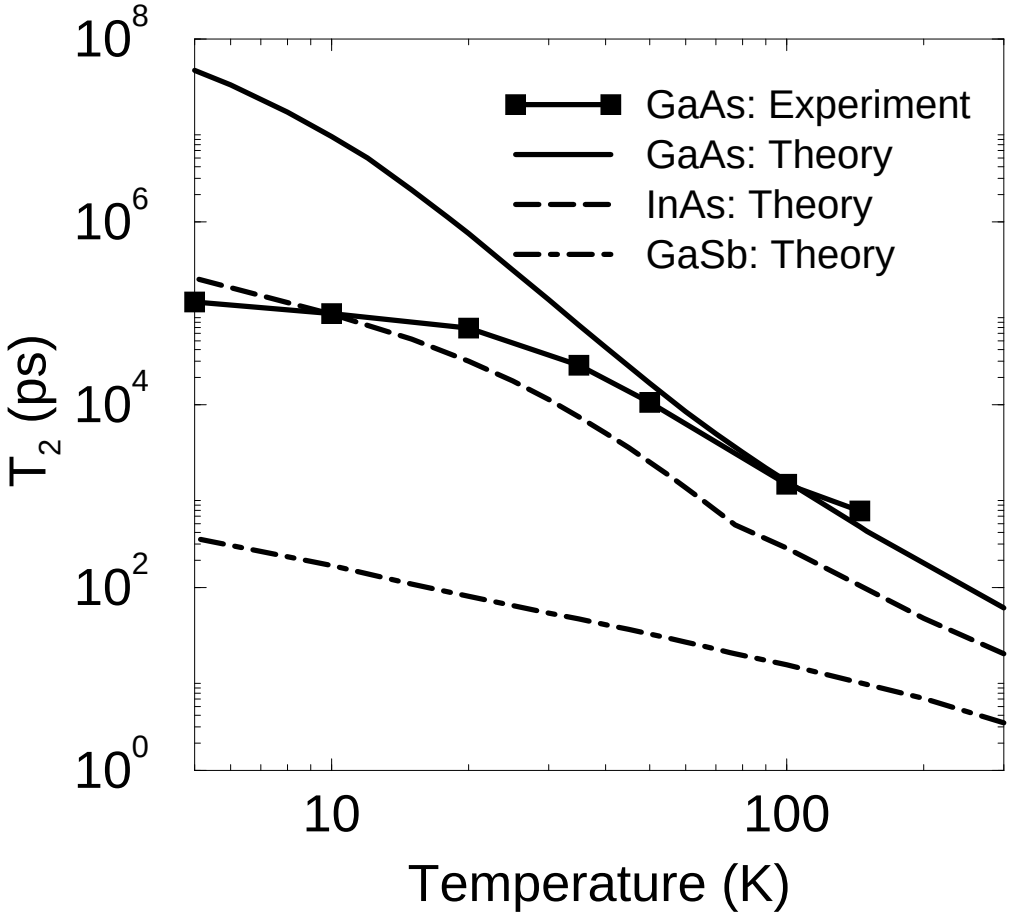

FIG. 1. T_2 in bulk III-V semiconductors as a function of temperature. Solid with squares and solid lines respectively represent the results of experiments [3] and the non-perturbative theory for bulk GaAs at the electron density $n = 1.0 \times 10^{16}$ cm^{-3}. Also shown are results for bulk InAs at $n = 1.7 \times 10^{16}$ cm^{-3} and bulk GaSb at $n = 1.49 \times 10^{18}$ cm^{-3}, which are indicated with dashed and dot-dashed lines respectively. The difference in slope between GaSb and GaAs occurs because GaSb is degenerate for this density. The tabulated mobilities [24] for InAs and GaSb extend only to 77K, so at lower temperatures $\tau_3(E)$ was assumed to have the same value as at 77K.

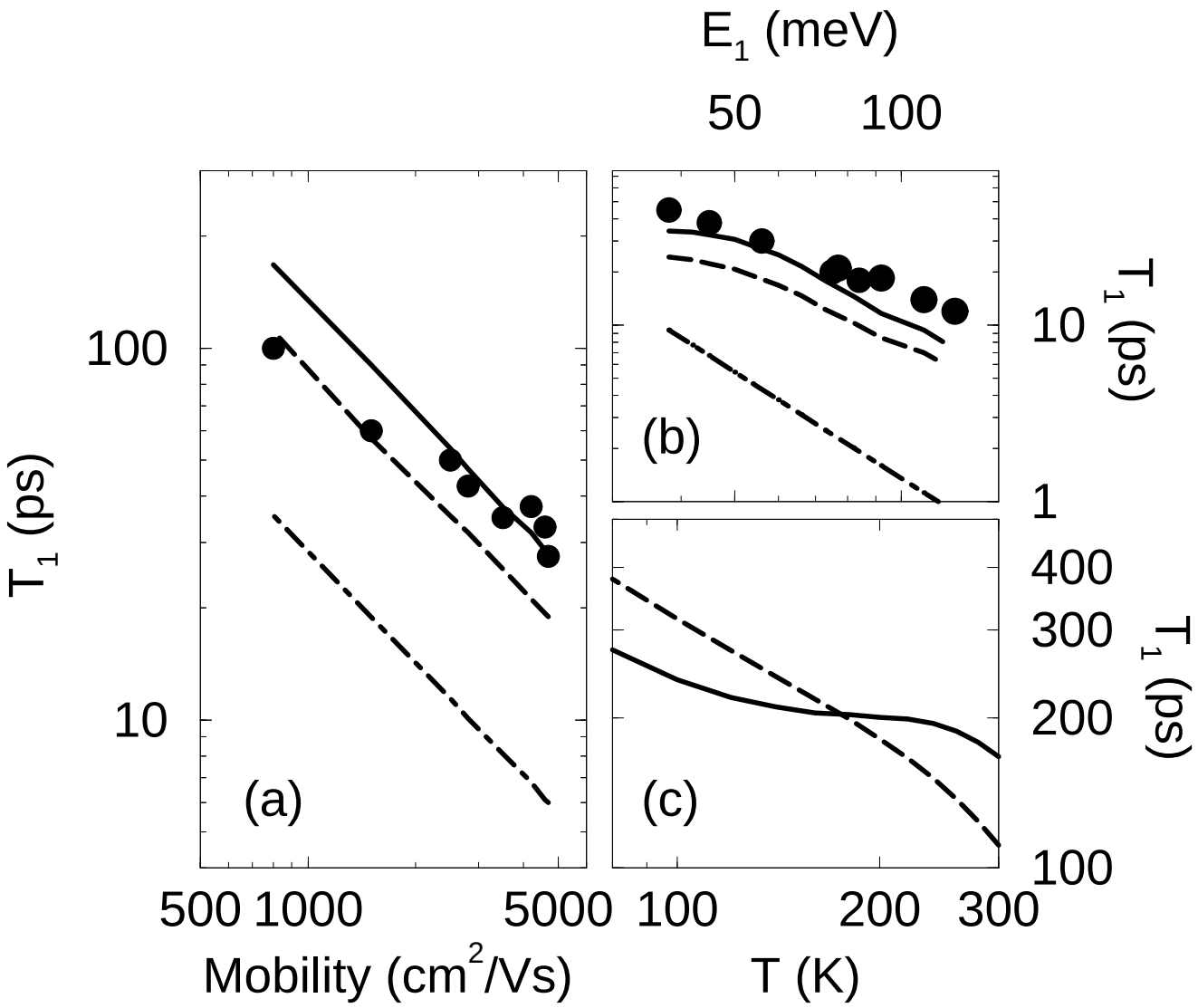

FIG. 2. T_1 as a function of (a) mobility, (b) confinement energy, and (c) temperature, for 75Å $GaAs/Al_{0.4}Ga_{0.6}As$ MQWs at room temperature. Closed circles represent the results of experiments [8]. The non-perturbative theory results with OP scattering (solid lines) and NI scattering (dashed lines) are shown, as well as the DK theory results (dot-dashed lines).

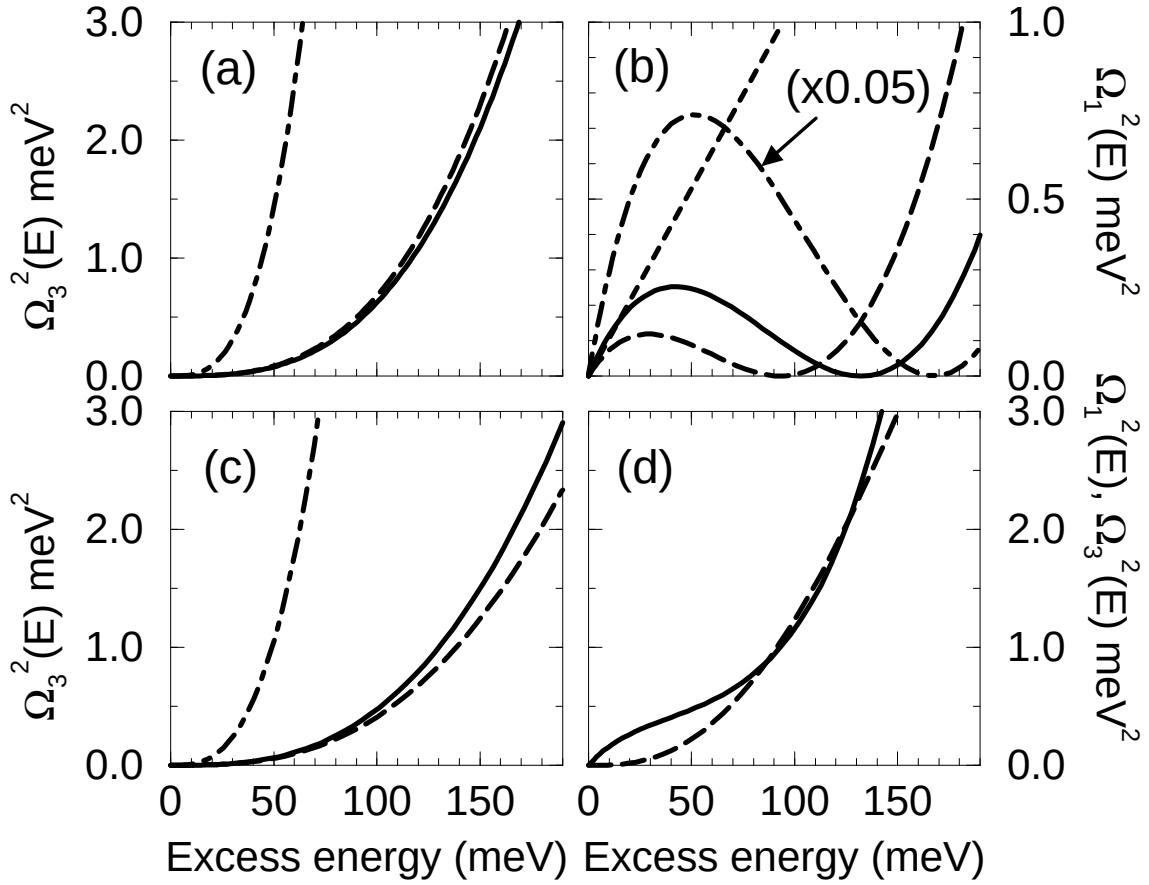

FIG. 3. $\Omega_1^2(E)$ and $\Omega_3^2(E)$ for several structures. (a) $\Omega_3^2(E)$ for bulk GaAs (solid), InAs (dashed), and GaSb (dot-dashed). (b) $\Omega_1^2(E)$ for GaAs (solid), InGaAs (long dashed), and GaSb (dot-dashed) quantum wells described in Table I. The short-dashed line is the DK approximation for the GaAs quantum well. (c) $\Omega_3^2(E)$ for the same three structures as (b). (d) $\Omega_1^2(E)$ (solid) and $\Omega_3^2(E)$ (dashed) for a thin-layer InAs/GaSb superlattice.